Onset Criteria for Bulk-Mode Thermoacoustic Instabilities in Supercritical Hydrocarbon Fuels

Steven A. Hunt[1,2]
School of Aeronautics and Astronautics,
Purdue University,
West Lafayette, IN 47907
e-mail: steven.hunt@virginorbit.com

Mario Tindaro Migliorino[3]
School of Mechanical Engineering,
Purdue University,
West Lafayette, IN 47907
e-mail: mariotindaro.migliorino@uniroma1.it

Carlo Scalo
School of Mechanical Engineering and Aeronautics and Astronautics (by courtesy),
Purdue University,
West Lafayette, IN 47907
e-mail: scalo@purdue.edu

Stephen D. Heister
School of Aeronautics and Astronautics,
Purdue University,
West Lafayette, IN 47907
e-mail: heister@purdue.edu

We have investigated supercritical-p ($p > 1192$ psi (8.22 MPa)) methanol at pressures up to 1645 psi (11.3 MPa) flowing through a heated tube at flow rates of 4–7 lb/h (1.8–3.2 kg/h). Tube heated lengths have been varied from 4 to 6 in (10 to 15 cm), internal diameters from 0.027 to 0.069 in (0.069 to 0.175 cm), and heat inputs between zero and 800 W. Fluid temperature at the tube inlet remained subcritical ($T < 464$ °F (513 K)); outlet temperatures were transcritical or supercritical. Two phenomena were observed: system-wide bulk-mode oscillations and localized acoustic modes. In this study, predictive efforts are undertaken to characterize system-wide bulk-mode oscillations. The parameter space has been nondimensionalized, yielding four dimensionless variables. Stability criteria based on these dimensionless groups have been established for two separate test articles and fluids; both criteria suggest that the heat required for the onset of oscillations is proportional to the mass flow rate times the mean pressure and inversely proportional to the fuel density.
[DOI: 10.1115/1.4049401]

Introduction

Increased combustion temperatures of modern gas turbine engines pose cooling issues for turbine blades. Many current engines flow cooling air through channels inside turbine blades, bled from the compressor. Cooling air can exit the compressor in excess of 1200 °F (900 K), which is cooler than the turbine blades. However, the blades could be more effectively cooled if the incoming air's temperature were reduced further by using the aircraft fuel as a heat sink. To achieve this, the high heat capacity of the relatively colder fuel can be exploited in a fuel–air heat exchanger upstream of the turbine [1]. In addition to improved turbine cooling, the resulting preheated fuel could improve the engine's combustion cycle efficiency [2]. However, large pressure oscillations have been known to occur within fuel flow paths [3–9], damaging or limiting life of heat exchanger components. Those oscillations were observed to occur for thermodynamic states close to the critical point, which exhibits drastic variations of all thermodynamic properties depending on the temperature, ranging from liquid-like to gas-like values. For this reason, the use of fuels at or near their critical temperature in fuel–air heat exchangers has been avoided. In order to fully exploit the fuel's cooling potential, engine manufacturers desire a model capable of predicting the onset of pressure oscillations.

Supercritical fuel oscillations occur with different modalities. Researchers have observed two distinct types of oscillations near the critical point: bulk-mode oscillations (also known as Helmholtz or pulsating oscillations) and acoustic-scale oscillations. Bulk-mode oscillations are characterized by high amplitudes and low frequencies (0.5–3 Hz), whereas acoustic oscillations are associated with low amplitudes and high frequencies (75–2000 Hz). A previous work by Hunt and Heister [10] compares test conditions and corresponding results from several publications.

Hines and Wolf [3] performed early experiments to study thermoacoustic oscillations in supercritical fuels. They tested turbulent flows of supercritical RP-1 and diethylcyclohexane (DECH) through thin-walled tubes designed to replicate flowpaths found in rocket cooling jackets. Oscillations were often audible in their tests; oscillations of well-defined frequency with constant amplitude caused a sound described as a "clear and steady scream," whereas oscillations with lower-frequency modulation exhibited "chugging or pulsing noises." Dominant frequencies and peak amplitudes encountered were in the range of 1000–7500 Hz and 50–380 psi, respectively. They unsuccessfully attempted to eliminate these oscillations by placing the tube in cement to damp the vibrations during a run.

Faith et al. [4] experimented with supercritical Jet-A fuel, flowing it through one of several types of resistively heated tubes. Tests were performed at mean pressures of up to 1000 psi. Heat input increased over a 5–10 min period until oscillations began, with heat flux values ranging from 0.02 to 4.0 BTU/sec in.^{2}. Oscillations manifested in the form of high-pitched noise. Pressure fluctuation amplitudes ranged up to 350 psi. Primary frequencies varied between 1000 and 5000 Hz.

Hitch and Karpuk [5] studied vertical flow of methylcyclohexane and JP-7 through a tube heated by band heaters. They observed two distinct types of oscillations near the critical point: Helmholtz/bulk-mode oscillations and acoustic oscillations. Helmholtz oscillations occurred with high amplitude at frequencies from 1 to 2 Hz, whereas acoustic oscillations occurred with low amplitude at higher frequencies of 75–450 Hz. Flows were always stable (i.e., no oscillatory response) when the fluid pressure was much higher than the critical pressure. Aiming to eliminate oscillations and increase heat transfer, Hitch and Karpuk tested several turbulating inserts: a twisted-tape insert, a louvered-tape insert, and a static mixer. All three inserts were found to increase the heat transfer coefficient. The static mixer caused the largest heat transfer improvement and reduced Helmholtz oscillations substantially. Flow stability could be maintained with a static mixer until pressure was reduced to less than 1.1 times the critical pressure. They successfully eliminated oscillations even below the critical pressure by using a damping valve to cause a flow restriction before the test section.

Linne et al. [6,7] performed a design of experiments to map out the stability of a flow and generated an empirical fit to discriminate between stable and unstable regions. Their tests involved

[1]Corresponding author.
[2]Present address: Virgin Orbit, 4022 E. Conant Street, Long Beach, CA 90808.
[3]Present address: Department of Mechanical and Aerospace Engineering, Sapienza University of Rome, Rome 00184, Italy.

Contributed by the Fluids Engineering Division of ASME for publication in the Journal of Fluids Engineering. Manuscript received March 5, 2020; final manuscript received October 22, 2020; published online January 18, 2021. Assoc. Editor: Gongnan Xie.

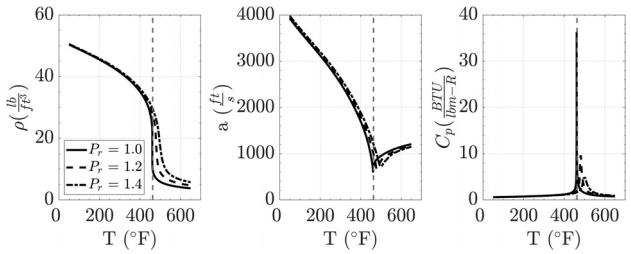

Fig. 1 Methanol density, ρ, speed of sound, a, and isobaric specific heat, c_p, versus temperature, T, from the NIST database [16]. The critical pressure of methanol is 1192 psi (8.22 MPa), and its critical temperature is 464 °F (513 K).

supercritical JP-7 fuel flowing through a vertical, resistively heated tube. Five independent variables were selected for this study: test section length, test section inner diameter, mass flow rate, inlet fluid temperature, and heat flux. Buoyancy was originally proposed as a driver of oscillations, but based on the Reynolds and Grashof numbers calculated, this effect was deemed negligible for all tests. The authors arbitrarily selected an root-mean-square pressure of 10 psi as the threshold between a stable and an unstable condition. A curve fit was generated, which correctly predicted some, but not all, test points as being stable or unstable. Moreover, the study did not test for applicability of substantially different upstream hardware or fluid types.

Herring's [1,8,11] research was aimed at developing a robust and high-performance fuel–air heat exchanger able to accept fuels near or above the supercritical point. Supercritical JP-10 flowed through a single resistively heated tube in his experimental tests. Independently varied parameters included inlet temperature, mass flow rate, input power, heated length, and total pipe length. This study also tested vertical and horizontal flows to determine the effect of buoyancy and several types of wire coil inserts in an attempt to improve heat transfer and suppress oscillations. Similar to the results of Hitch and Karpuk, Herring observed bulk-mode oscillations for reduced pressures up to 1.5. Like many other experiments, oscillations were observed only when the wall temperature was above the critical temperature, and the fuel inlet temperature was subcritical. Unlike the results of Hitch and Karpuk [5], however, the use of an upstream damping valve did not prevent bulk-mode oscillations. Herring postulated that this was due to the different flow systems used: Hitch and Karpuk used a pump-fed system, so the upstream pressure of the fluid was directly controlled, as opposed to Herring (and Linne) who pressurized gaseous N2 to drive the flow. In the latter approach, compressibility effects are observed in the ullage of the source tank, resulting in oscillations of the liquid flow rate.

Attempts at deriving a predictive criterion for the onset of bulk-mode thermoacoustic oscillations are scarce in the literature [7,12–14]. Only recently, a dimensionless criterion based on the density difference between fuel in the mainstream and fuel near the wall was developed [13]. The objective of this study is to develop criteria based on the Buckingham Pi theorem to predict the onset of bulk-mode thermoacoustic instabilities under conditions relevant to hydrocarbon-based aviation fuel systems [15]. In order to safely and more inexpensively perform experiments, a surrogate fluid was employed, and a range of variables believed to influence thermoacoustic oscillations were examined.

Facility Description

Bulk-mode oscillations were observed to be related to large property changes (e.g., density, conductivity, viscosity, heat capacity) that occur near the critical point. For this reason, supercritical methanol is chosen for this study (see Fig. 1 with data obtained from Refs. [16] and [17]) as a surrogate for a hydrocarbon-based aviation fuel. The steep density slope in the neighborhood surrounding the critical temperature indicates a transition known as "pseudo-boiling" or "pseudo-condensation" because formal phase changes are not occurring; however, bulk property changes mimic those occurring from boiling or condensation. This transitioning process has also been shown to affect thermoacoustic instabilities [18] and heat-induced shock waves [19] in previous numerical studies and is exploited here experimentally to investigate bulk-mode oscillations.

Figure 2 is a summary of the main facility hardware. Methanol test fluid is loaded into the run tank and pressurized with nitrogen. A pneumatic valve is used to connect or disconnect the methanol tank with the test section. A Coriolis flowmeter between the tank and pneumatic valve measures the mass flow rate of the test fluid. The fluid continues to a filter and then an electric preheater, which consists of an array of tubes sandwiched by copper blocks heated with cartridge heaters. The preheated fuel then enters the test section, which consists of a tube undergoing electric resistance heating. The test section is electrically insulated on each end with isolation flanges. Downstream of the test section, the fluid passes through a cooling bath, filter, flow control valve, sampling station, and finally a waste drum. A manual valve provides nitrogen for purging the test section.

Type K thermocouples were mounted in both the inlet and outlet plenums. The tubes tested were too small to accommodate thermocouples, so only outer wall temperatures were measured along the test section. Ungrounded thermocouples were selected despite their relatively slow response times in order to minimize instrumentation noise from the resistively heated tube. Thermocouple locations are shown in Fig. 2 as annotations with the letter

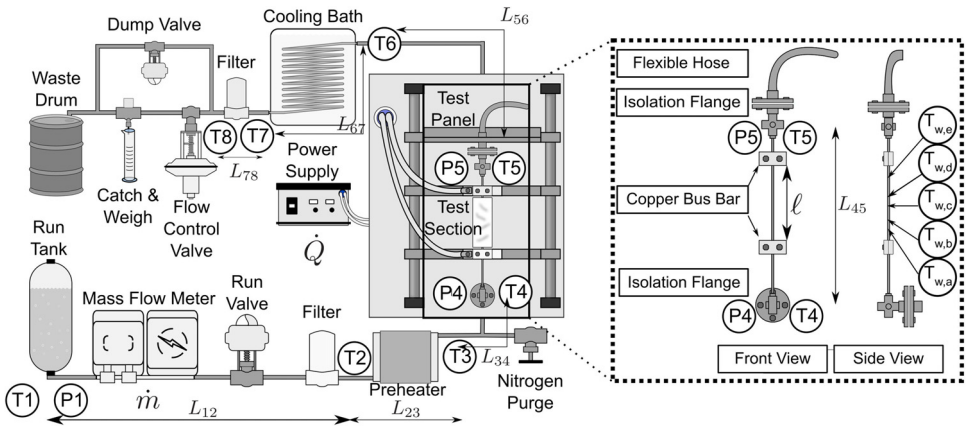

Fig. 2 Overall facility schematic; quantities defined in Tables 1 and 2. Wall temperatures designated with a w subscript; fluid temperatures designated with no subscript.

Table 1 Testing matrix for methanol

Test parameters			
Heated length	ℓ	in.	4, 6
Tube O.D.	Dout	in.	0.125
Tube I.D.	Din	in.	0.027, 0.069, 0.093
Reduced pressure	pr		1.0, 1.2, 1.4
Mass flow	$\dot{m}$	lbm/h	4, 5, 6, 7
Heat input	$\dot{Q}$	W	0–800

Table 2 Distances along fuel flow path

Flow lengths		
Tank to preheater	L_{12}	6 ft
Preheater inlet to exit	L_{23}	16 in.
Preheater exit to test section inlet	L_{34}	22 in.
Test section inlet to outlet	L_{45}	9.5 or 11 in.
Test section outlet to cooling bath inlet	L_{56}	21 in.
Cooling bath inlet to exit	L_{67}	80 ft
Cooling bath exit to control valve	L_{78}	2 ft

T. Wall temperatures are designated with a w subscript; fluid temperatures are designated with no subscript.

Kulite ETL-GTS-190 (M) (Leonia, NJ) pressure transducers were placed in the inlet and outlet plenum. These transducers are rated to temperatures up to 1025 °F and pressures of 3000 PSI. The special high frequency amplifier allows the transducer to be used up to 150 kHz. Data recorded during experiments were sampled at 4 kHz. Pressure transducer locations are shown in Fig. 2 as annotations with the letter P. Table 1 lists values for parameters varied throughout the experiments. The chosen reduced pressures ($p_r = p/p_{\text{crit}}$) of 1.0, 1.2, and 1.4 correspond to pressures of 1175, 1410, and 1645 psi. Table 2 lists distances between major components of the experiment.

Measurements

Unfiltered pressure and wall temperature traces obtained near the test section and tank, as well as a mass flow rate trace, are shown in Fig. 3 for a selected case. Wall temperature fluctuations (Fig. 4) and time-averaged fluid temperatures throughout the flow path and test section outer wall temperatures (Fig. 5) are also shown for the same case. Seven probes were evenly spaced along the tube; however, the fifth and sixth thermocouples from the inlet failed, so results from the seventh have been assigned to T_{we}. Fluid temperatures measured at the heated tube inlet and exit are also included. Bulk fluid temperatures in the case depicted by Figs. 3–5 remained subcritical throughout the flow path. The critical temperature acts as a natural boundary due to the high specific heat associated with these conditions, illustrated in Fig. 1. However, in some cases throughout the test campaign, sufficient energy was imparted to the fluid to reach supercritical bulk temperatures.

Oscillations are most prominently displayed in pressure traces near the test section tube and the mass flow rate measurements. Throughout the test campaign, similar to previous studies, two modes of oscillations were detected: the acoustic mode, characterized by frequencies of 360–581 Hz; and the bulk mode, characterized by frequencies from 1 to 5 Hz. Bulk mode oscillations, which are the main focus of this study, tend to have amplitudes of over one order of magnitude larger than the acoustic mode. The case illustrated in Figs. 3–5 is representative of the test campaign; both oscillation modes are present, but the bulk mode dominates. Mass flow rate oscillates in phase with pressures p_4 and p_5, which suggests that the instability is a system-wide phenomenon. Bulk-mode oscillations are visible in some wall temperature traces, but the amplitudes here are much smaller than those in the tube

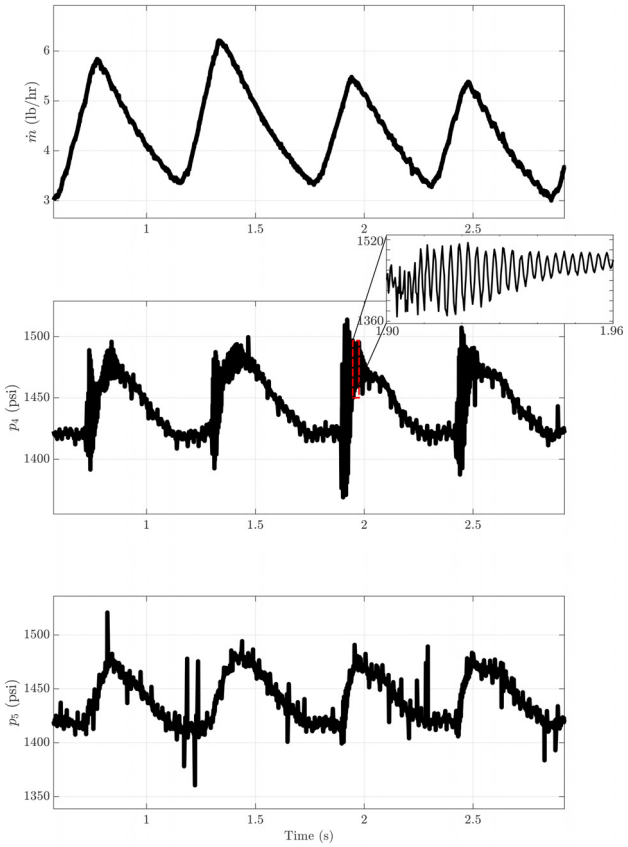

Fig. 3 Unfiltered mass flow rate, tank pressure, and tube inlet pressure of a selected case: $\dot{Q}$ = 550 W, D_{in} = 0.069 in., ℓ = 6 in., $\dot{m}$ = 5 lb/h, p_r = 1.2

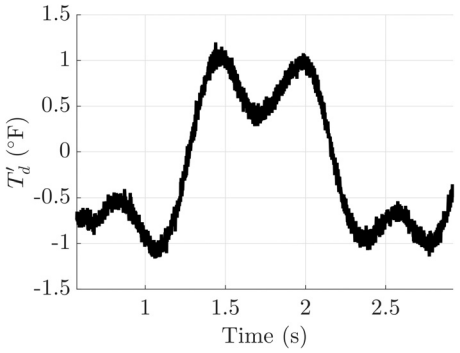

Fig. 4 Test section wall temperature fluctuations for a selected case: $\dot{Q}$ = 550 W, D_{in} = 0.069 in., ℓ = 6 in., $\dot{m}$ = 5 lb/h, p_r = 1.2. High-frequency noise is present, and unrelated to bulk-mode oscillations.

pressure and mass flow rate. These wall temperature signals undergo damping and lag due to the thermal resistance of the stainless steel tube. The bulk-mode is not well-displayed by thermocouples located anywhere in the flow-path; this may be because the thermocouples are located in wide plenums in which significant mixing occurs, interfering with the temperature oscillations.

A proposed driving mechanism for bulk-mode oscillations, which also aided in the formulation of a stability criterion, is as follows. The oscillation cycle begins with both mass flow rate and pressure near minimum values. At this time, the periodic process has cooled the tube wall to the point where a continuous flow of pseudo-liquid is present in the heated section. However, as the external heat input is nearly constant, the fluid layer nearest to the

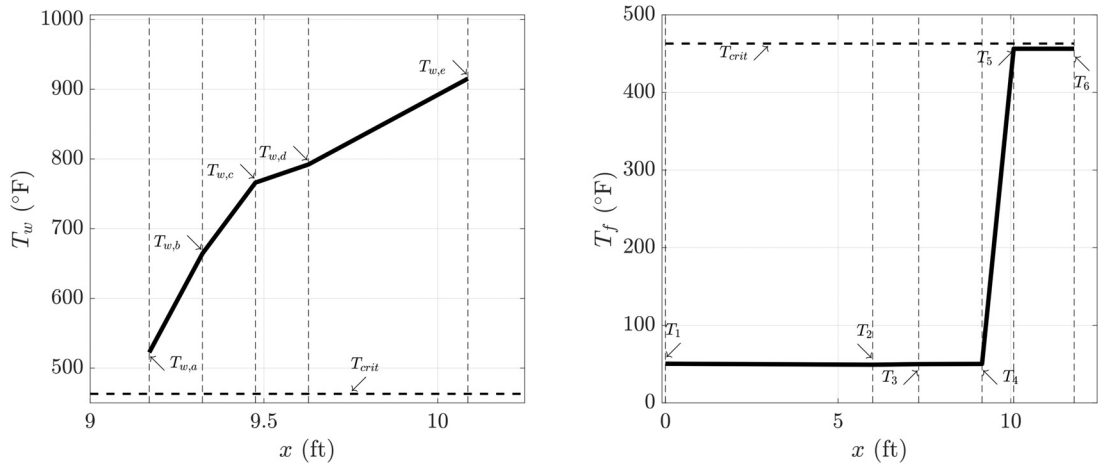

Fig. 5 Time-averaged wall (left) and bulk fluid (right) temperatures for a selected case: $\dot{Q} = 550$ W, $D_{in} = 0.069$ in., $\ell = 6$ in., $\dot{m} = 5$ lb/h, $p_r = 1.2$

wall, starting from the downstream section, is heated past its pseudo-boiling point and begins to expand toward the center of the tube. As a result, the pseudo-gas volume fraction increases. Smaller tube diameter, increased heat input, and decreased mass flow rate are all conducive to greater pseudo-gas fractions. At this time, mass flow rate through the tube is severely limited due to low-density pseudo-gas inhibiting the upstream flow of high-density pseudo-liquid. This is accentuated near the critical point, creating a dramatic increase in pressure due to the pseudo-vapor lock of the flow path. Pressure rises until a critical threshold is reached allowing for the rapid flushing of the largely pseudo-gaseous mixture from the heated section. As the upstream pressure is relieved, mass flow rate is decreased, allowing the process to repeat. It should be noted that there are other types of instabilities with similar outward appearance, such as chugging oscillations observed in liquid rocket engines [20] and density wave oscillations found in two-phase flow [21]; however, these oscillation modes are characterized by different underlying physics.

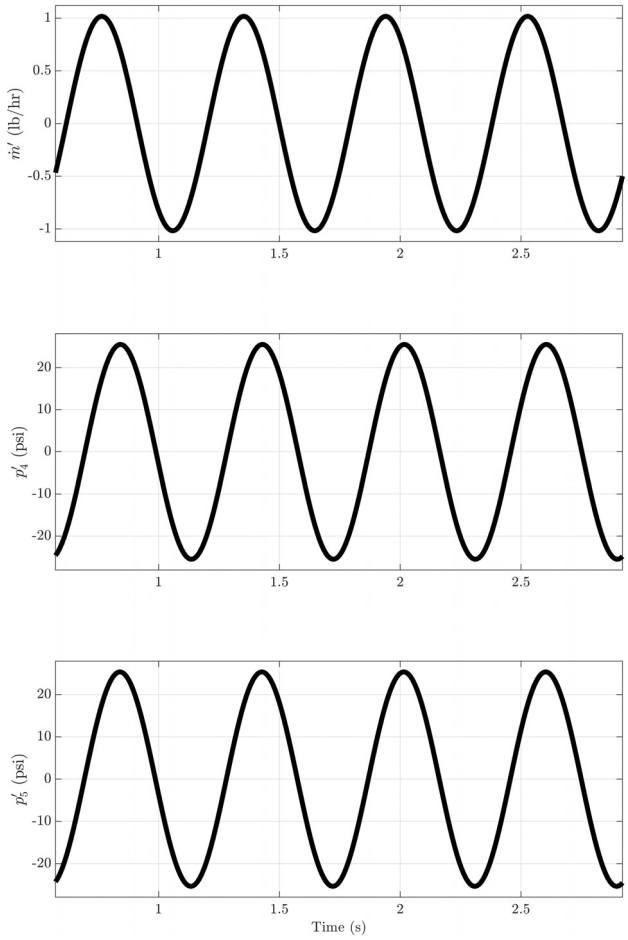

Fig. 6 Filtered mean-subtracted mass flow rate, tank pressure, and tube inlet pressure of a sample selected case: $\dot{Q} = 550$ W, $D_{in} = 0.069$ in., $\ell = 6$ in., $\dot{m} = 5$ lb/h, $p_r = 1.2$

Data Analysis

From the 175 test cases taken from the thesis of Palumbo [9], 88 test cases with strong and consistent pressure oscillations having distinct major frequencies were chosen for analysis. Bulk-mode oscillations dominate pressure and mass flow rate traces such as those depicted by Fig. 3 and are therefore the subject of this study. However, oscillations due to the acoustic mode, hydrodynamics and instrumentation noise were also present in these data. These signals were filtered, leaving only the strongest oscillation mode in the processed signal. These filtered signals, with mean values subtracted, are shown in Fig. 6.

Data from the test article have been analyzed to determine thresholds of several flow parameters for the occurrence of oscillations. Independent variables include mean pressure ($\bar{p}$), fuel mass flow rate ($\dot{m}$), heated tube diameter (D_{in}), heat input ($\dot{Q}$), fuel density (ρ), and fuel viscosity (μ). Density and viscosity were considered at the heated tube inlet. The dependent variable was the pressure amplitude of the bulk mode. A nondimensional analysis was performed in the interest of finding a range of all

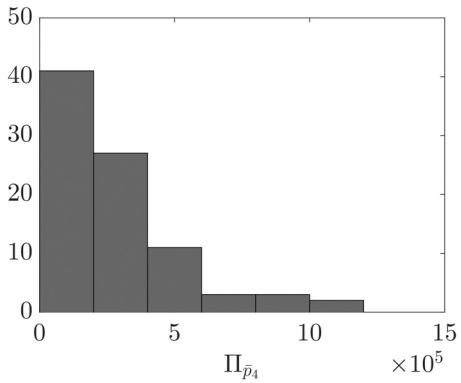

Fig. 7 Histogram of all values of $\Pi_{\bar{p}_4}$ in dataset

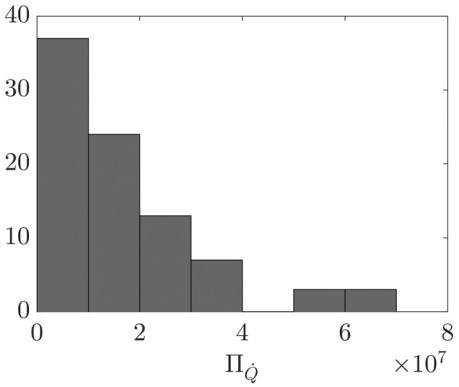

Fig. 8 Histogram of all values of $\Pi\dot{Q}$ in dataset

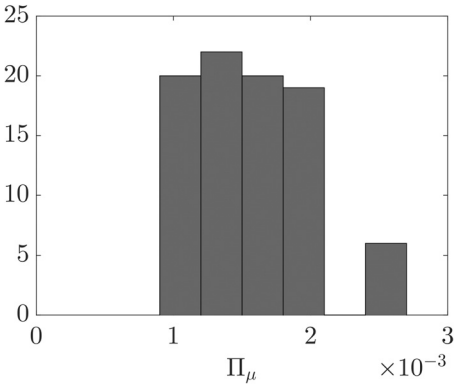

Fig. 9 Histogram of all values of Π_{μ} in dataset

independent variables that is nonconducive to oscillations. The Buckingham Pi theorem yielded four dimensionless groups

$$\Pi_{\bar{p}_4} = \frac{D_{\text{in}}^4 \rho \bar{p}}{\dot{m}^2} \qquad \Pi_{p_{4,\text{amp}}} = \frac{D_{\text{in}}^4 \rho p_{\text{amp}}}{\dot{m}^2}$$
$$\Pi\dot{Q} = \frac{D_{\text{in}}^4 \rho^2 \dot{Q}}{\dot{m}^3} \qquad \Pi_{\mu} = \frac{D_{\text{in}} \mu}{\dot{m}} \propto \frac{1}{\text{Re}_D} \tag{1}$$

The significance of these dimensionless groups is as follows:

(1) $\Pi_{\bar{p}_4}$ relates mean pressure to the dynamic pressure of the mean flow.
(2) $\Pi_{p_{4,\text{amp}}}$, the only output group, relates pressure oscillation amplitude and dynamic pressure.
(3) $\Pi\dot{Q}$ relates thermal and kinetic energy transport.
(4) Π_{μ} acts like the Reynolds number for internal flow, relating viscous forces, and inertial forces.

The values of each of the input dimensionless groups are plotted in Figs. 7–9. $\Pi_{\bar{p}_4}$ and $\Pi\dot{Q}$ both span several orders of magnitude, whereas Π_{μ} remains relatively unchanged throughout the dataset. Figure 10 relates $\Pi_{p_{4,\text{amp}}}$ (dimensionless pressure amplitude) to $\Pi\dot{Q}$ (dimensionless heat input). Each series in the plot represents a range of $\Pi_{\bar{p}_4}$ (dimensionless mean pressure) values; the median of each $\Pi_{\bar{p}_4}$ range is denoted on the legend. Logarithmic curve fits were applied to these series. All values of Π_{μ} (inverse Reynolds number) were included in the plot indiscriminately, as the entire range of its values was relatively small. Unsurprisingly, the oscillation amplitude group tends to increase as the power input group increases. A test case is considered stable if $\Pi_{p_{4,\text{amp}}}$, the dimensionless group representing pressure amplitude, is near zero. Therefore, for each $\Pi_{\bar{p}_4}$ curve, the location of the x intercept represents the threshold dimensionless power input required for oscillations to occur. This threshold power increases monotonically with the increasing $\Pi_{\bar{p}_4}$ (dimensionless mean pressure) values.

A predictive stability criterion, shown in Eq. (2), quantifies the onset dimensionless power for oscillations as a function of dimensionless mean pressure

$$\Pi_{\dot{Q},\text{onset}} = f(\Pi_{\bar{p}_4}) \tag{2}$$

Figure 11 plots $\Pi_{\dot{Q},\text{onset}}$ (onset dimensionless power) for several values of $\Pi_{\bar{p}_4}$ (dimensionless mean pressure). Operating points beneath this curve would be predicted as stable, and those above would be predicted to exhibit oscillations. A power-law regression for $\Pi_{\dot{Q},\text{onset}}$ versus $\Pi_{\bar{p}_4}$, is shown in the following equation:

$$\Pi_{\dot{Q},\text{onset}} = 8.643\Pi_{\bar{p}_4}^{1.155} - 2.945 \times 10^6 \tag{3}$$

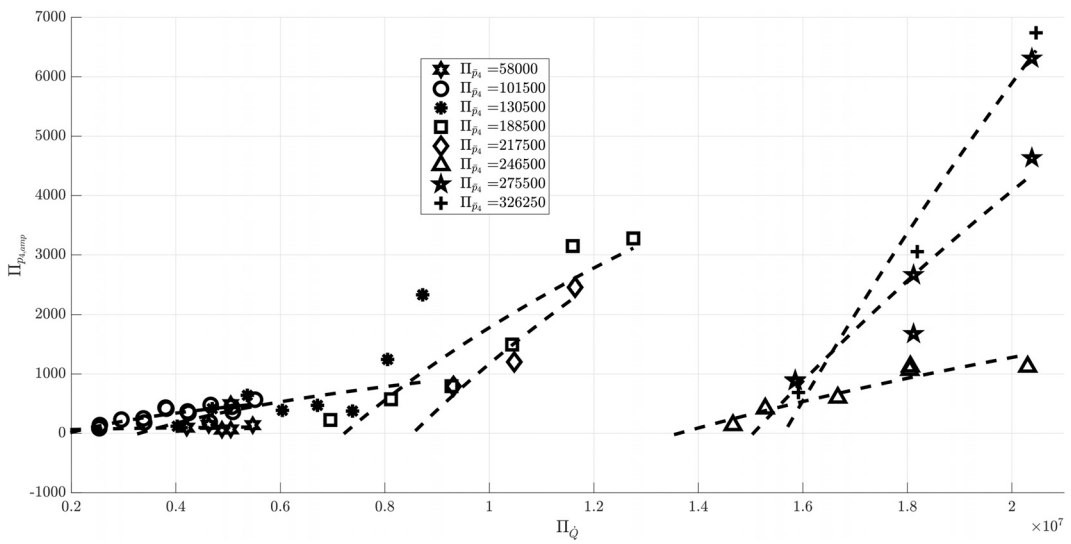

Fig. 10 Dimensionless pressure amplitude versus dimensionless heat input. Dashed lines represent curve fits for each dimensionless mean pressure bin.

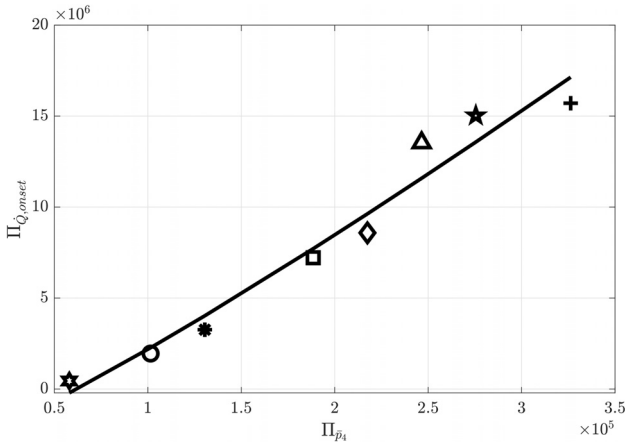

Fig. 11 Onset dimensionless heat input versus dimensionless mean pressure

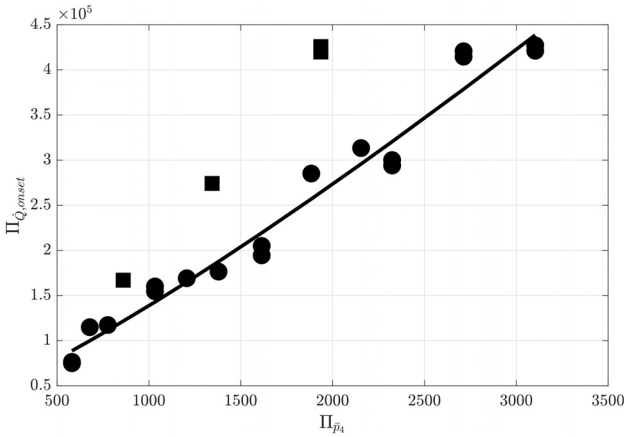

Fig. 12 Onset dimensionless heat input versus dimensionless mean pressure for all 24 nonpreheated cases from Wang et al. [12] Cases performed at $p = 2.5$ MPa (reduced pressure of 1.09) are designated by squares; all others are designated with circles.

A linear regression for $\Pi_{\dot{Q},\text{onset}}$ versus $\Pi_{\bar{p}_4}$, in which the y-intercept is forced to equal zero, is shown in the following equation:

$$\Pi_{\dot{Q},\text{onset}} = 46.2\Pi_{\bar{p}_4} \tag{4}$$

Substituting variables for the dimensionless groups and canceling like terms yields the approximate critical heat input as a function of mean pressure, mass flow rate, and fluid density

$$\dot{Q}_{\text{onset}} = 46.2\frac{\bar{p}\dot{m}}{\rho} \tag{5}$$

where $\dot{Q} < \dot{Q}_{\text{onset}}$ predicts a stable (nonoscillatory) flow.

The worst-case bias errors of critical onset heat input and dimensionless groups were calculated with consideration to bias errors present in the hardware used. Because outputs were sampled many times for each recording, precision error was assumed negligible and was ignored for the uncertainty analysis. Π_μ was omitted from this uncertainty analysis due to its invariance in the stability criteria. The worst-case bias errors of $\Pi_{\bar{p}_4}$, $\Pi_{p_{4,\text{amp}}}$, and $\dot{Q}_{\text{onset}}$ were 6.551×10^5, 6.340×10^5, and 41.72 W, respectively.

Onset Criteria for RP-3 Fuel

Wang et al. [12] heated RP-3 to supercritical temperatures and investigated thermoacoustic oscillations therein. The method of generating a stability criterion discussed in the Data Analysis section shall be used with the dataset reported by Wang et al. Cases with preheating were excluded from this analysis in the interest of obtaining accurate heat transfer measurements throughout the system. Figure 12 depicts $\Pi_{\dot{Q},\text{onset}}$ (onset dimensionless power) versus $\Pi_{\bar{p}_4}$ (dimensionless mean pressure). Operating points beneath this curve would be predicted as stable, and those above would be predicted to exhibit oscillations. Although a trend is evident, notable outliers are cases run with $p = 2.5$ MPa, which was the lowest pressure setting run by Wang et al. This pressure corresponds to a reduced pressure of 1.09. These five points, designated by squares in Fig. 12, were excluded from the curve fit. The remaining 19 points, designated by circles, produced a much stronger trend. Several factors may prevent the stability analysis from correctly predicting the threshold power for low-pressure cases. The fuel may have unintentionally been pressurized to a subcritical pressure in the lowest-pressure setting cases, due to either abnormal fuel composition or pressure transducer error. Although this cannot be proven, the behavior does match that which may be expected with subcritical-p fluids: the fluid remains stable throughout the liquid phase but will eventually exhibit instabilities once sufficient power is input to boil a significant amount of the fuel. The energy required to undergo actual boiling is larger than that required for pseudo-boiling.

A power-law regression for $\Pi_{\dot{Q},\text{onset}}$ versus $\Pi_{\bar{p}_4}$ for Wang et al.'s data is shown in the following equation:

$$\Pi_{\dot{Q},\text{onset}} = 27.29\Pi_{\bar{p}_4}^{0.7186} - 3.412 \times 10^4 \tag{6}$$

A linear regression for $\Pi_{\dot{Q},\text{onset}}$ versus $\Pi_{\bar{p}_4}$, in which the y-intercept is forced to equal zero, is shown in the following equation:

$$\Pi_{\dot{Q},\text{onset}} = 139.1\Pi_{\bar{p}_4} \tag{7}$$

Substituting variables for the dimensionless groups and canceling like terms yields the approximate maximum heat input for nonoscillating flow as a function of mean pressure, mass flow rate, and fluid density. This relation is given in the following equation:

$$\dot{Q}_{\text{onset}} = 139.1\frac{\bar{p}\dot{m}}{\rho} \tag{8}$$

Despite the general behavior of each correlation being the same (onset dimensionless power scales nearly linearly with dimensionless mean pressure), it is not expected for the correlations to match exactly between test articles. These two correlations merely differ by their coefficients. This coefficient may be a function of variables not captured within the dimensionless groups selected, such as flow path geometry (viz., tube length or heated length) or fluid properties. More experiments would need to be performed in order to determine how to predict this coefficient.

Conclusions

Thermoacoustic oscillations have been detected in upward flow of methanol through a heated test section. The amplitude of the pressure oscillations was observed to depend on mass flow rate, diameter of the heated section, mean pressure, and heat input. A novel dimensionless scaling technique allows to fit experimental data both from this work and from the literature. The potential of this technique is to predict the onset of bulk-mode thermoacoustic oscillations in heat exchangers using supercritical fluids with a simple and inexpensive model.

Acknowledgment

The guidance of Patrick C. Sweeney is gratefully acknowledged.

Funding Data

- This work has been funded by Rolls-Royce Corporation Indianapolis (Funder ID: 10.13039/501100000767).
- M. T. Migliorino also acknowledges the support of the Frederick N. Andrews Doctoral Fellowship at Purdue University.

References

[1] Herring, N. R., and Heister, S. D., 2006, "Review of the Development of Compact, High Performance Heat Exchangers for Gas Turbine Applications," ASME Paper No. IMECE2006-14920.
[2] Wiest, H., Larson, L., Heister, S. D., and Meyer, S., 2013, "Experimental Study of Gas Turbine Combustion With Elevated Fuel Temperatures," AIAA Paper No. 2013-3689.
[3] Hines, W. S., and Wolf, H., 1962, "Pressure Oscillations Associated With Heat Transfer to Hydrocarbon Fluids at Supercritical Pressures and Temperatures," ARS J., **32**(3), pp. 361–366.
[4] Faith, L. E., Ackerman, G. H., and Henderson, H. T., 1971, "Heat Sink Capability of Jet a Fuel: Heat Transfer and Coking Studies," NASA, Reston, VA, Report No. CR-72951.
[5] Hitch, B., and Karpuk, M., 1998, "Enhancement of Heat Transfer and Elimination of Flow Oscillations in Supercritical Fuels," AIAA Paper No. 98-3759.
[6] Linne, D., Meyer, M., Edwards, T., and Eitman, D., 1997, "Evaluation of Heat Transfer and Thermal Stability of Supercritical JP-7 Fuel," AIAA Paper No. 97-3041.
[7] Linne, D., Meyer, M., Braun, D., and Keller, D., 2000, "Investigation of Instabilities and Heat Transfer Phenomena in Supercritical Fuels at High Heat Flux and Temperatures," AIAA Paper No. 2000-3128.
[8] Herring, N. R., 2007, "On the Development of Compact, High Performance Heat Exchangers for Gas Turbine Applications," Ph.D. thesis, Purdue University, West Lafayette, IN.
[9] Palumbo, M., 2009, "Predicting the Onset of Thermoacoustic Oscillations in Supercritical Fluids," Master's thesis, Purdue University, West Lafayette, IN.
[10] Hunt, S., and Heister, S. D., 2014, "Thermoacoustic Oscillations in Supercritical Fuel Flows," AIAA Paper No. 2014-3973.
[11] Herring, N. R., and Heister, S. D., 2009, "On the Use of Wire-Coil Inserts to Augment Tube Heat Transfer," J. Enhanced Heat Transfer, **16**(1), pp. 19–34.
[12] Wang, H., Zhou, J., Pan, Y., and Wang, N., 2015, "Experimental Investigation on the Onset of Thermo-Acoustic Instability of Supercritical Hydrocarbon Fuel Flowing in a Small-Scale Channel," Acta Astronaut., **117**, pp. 296–304.
[13] Pan, H., Bi, Q., Liu, Z., Feng, S., and Feng, F., 2018, "Experimental Investigation on Thermo-Acoustic Instability and Heat Transfer of Supercritical Endothermic Hydrocarbon Fuel in a Mini Tube," Exp. Therm. Fluid Sci., **97**, pp. 109–118.
[14] Wang, Y., Li, S., and Dong, M., 2019, "Experimental Investigation on Heat Transfer Deterioration and Thermo-Acoustic Instability of Supercritical-Pressure Aviation Kerosene Within a Vertical Upward Circular Tube," Appl. Therm. Eng., **157**, p. 113707.
[15] Sweeney, P. C., Heister, S. D., Hunt, S. A., Scalo, C., and Migliorino, M. T., 2017, "System and Method for Stabilizing Transcritical Air-to-Fuel Heat Exchange," U.S. Patent Application No. 15/473,759.
[16] Lemmon, E. W., McLinden, M. O., and Friend, D. G., 2019, *Thermophysical Properties of Fluid Systems in NIST Chemistry WebBook, NIST Standard Reference Database Number 69*, National Institute of Standards and Technology, Gaithersburg, MD, p. 20899.
[17] Huber, M., 2003, "NIST Thermophysical Properties of Hydrocarbon Mixtures Database (SUPERTRAPP)," U.S. Department of Commerce, National Institute of Standards and Technology, Gaithersburg, MD.
[18] Migliorino, M. T., and Scalo, C., 2020, "Real-Fluid Effects on Standing-Wave Thermoacoustic Instability," J. Fluid Mech., **883**, p. A23.
[19] Migliorino, M. T., and Scalo, C., 2020, "Heat-Induced Planar Shock Waves in Supercritical Fluids," Shock Waves, **30**(2), pp. 153–167.
[20] Heister, S. D., Anderson, W. E., Pourpoint, T. L., and Cassady, R. J., 2019, "Rocket Propulsion," *Cambridge Aerospace Series*, Cambridge University Press, Cambridge, UK.
[21] O'Neill, L. E., and Mudawar, I., 2018, "Mechanistic Model to Predict Frequency and Amplitude of Density Wave Oscillations in Vertical Upflow Boiling," Int. J. Heat Mass Transfer, **123**, pp. 143–171.